

# Relic neutrino detection through angular correlations in inverse $\beta$ -decay

**Evgeny Akhmedov**

Max-Planck-Institut für Kernphysik, Saupfercheckweg 1,  
69117 Heidelberg, Germany

E-mail: [akhmedov@mpi-hd.mpg.de](mailto:akhmedov@mpi-hd.mpg.de)

**Abstract.** Neutrino capture on beta-decaying nuclei is currently the only known potentially viable method of detection of cosmic background neutrinos. It is based on the idea of separation of the spectra of electrons or positrons produced in captures of relic neutrinos on unstable nuclei from those from the usual  $\beta$ -decay and requires very high energy resolution of the detector, comparable to the neutrino mass. In this paper we suggest an alternative method of discrimination between neutrino capture and  $\beta$ -decay, based on periodic variations of angular correlations in inverse beta decay transitions induced by relic neutrino capture. The time variations are expected to arise due to the peculiar motion of the Sun with respect to the  $C\nu B$  rest frame and the rotation of the Earth about its axis and can be observed in experiments with both polarized and unpolarized nuclear targets. The main advantage of the suggested method is that it does not depend crucially on the energy resolution of detection of the produced  $\beta$ -particles and can be operative even if this resolution exceeds the largest neutrino mass.

---

## Contents

<b>1</b>	<b>Introduction</b>	<b>1</b>
<b>2</b>	<b>Neutrino capture in inverse <math>\beta</math> decay</b>	<b>4</b>
2.1	Gamow-Teller $1^\pi \rightarrow 0^\pi$ transitions	4
2.2	Neutrino capture on unpolarized nuclei	6
2.3	Comparison with $\nu$ capture on polarized tritium ( $1/2^+ \rightarrow 1/2^+$ )	8
<b>3</b>	<b>Implications for relic neutrino capture: lab frame</b>	<b>8</b>
3.1	Polarized targets	10
3.2	Unpolarized targets	12
<b>4</b>	<b>Separation of periodic signal from large fluctuating background</b>	<b>12</b>
<b>5</b>	<b>Discussion</b>	<b>18</b>
<b>A</b>	<b>Angular averaging</b>	<b>19</b>
<b>B</b>	<b>Electron asymmetry with respect to a fixed direction in the lab frame</b>	<b>20</b>

---

## 1 Introduction

Standard cosmology predicts the existence of a sea of active left-handed neutrinos and their right-handed antiparticles that decoupled from the cosmic plasma at temperatures  $T \sim 2$  MeV and have cooled down in the course of the expansion of the Universe [1–3]. At present, these cosmic background neutrinos ( $C\nu B$ ) are expected to have nearly Fermi-Dirac spectrum with the temperature  $T_{\nu 0} \simeq 1.945 \text{ K} \simeq 1.676 \times 10^{-4} \text{ eV}$  and to be in states of definite mass rather than in flavour states [4]. Together with data from neutrino oscillation experiments, this, in particular, means that at least two relic neutrino species must be non-relativistic at the present epoch. Because of their extremely low energies and the weak nature of neutrino interactions, the relic neutrinos have not yet been directly detected. At the same time, they should carry rich and important information about the very early stages of the evolution of the Universe; their observation thus represents one of the main challenges of modern cosmology. Detection of relic neutrinos may also shed light on some important neutrino properties, such as their Dirac vs. Majorana nature and possible existence of light sterile neutrinos.

Several approaches to detecting the  $C\nu B$  neutrinos have been suggested to date, see e.g. refs. [5–7] for reviews. Unfortunately, most of them either were based on flawed considerations or are rather impractical. Out of all the suggestions put forward so far, only neutrino capture on beta-decaying nuclei has a chance to bear fruit in a foreseeable future. As this process is threshold-free, even neutrinos of extremely low energies can be captured with finite rate. The approach is based on separation of the spectra of  $\beta$ -particles produced in capture of relic neutrinos from those coming from the usual  $\beta$ -decay of the target nuclei. It was first suggested by Weinberg back in 1962 in the context of massless relic neutrinos with large chemical potential  $\xi$  [8]. However, current stringent limits on  $\xi$  rule out this possibility.

The idea of using neutrino capture on beta-decaying nuclei for detecting  $C\nu B$  neutrinos was revived in a modern setting by Cocco et al. [9], who noted that, as the neutrinos

are actually massive, the spectrum of  $\beta$ -particles produced in captures of relic neutrinos of mass  $m_\nu$  must be separated from the spectrum of the much more abundant electrons or positrons coming from the usual  $\beta$  decay of the target nuclei by a gap  $\sim 2m_\nu$  (assuming  $m_\nu \gtrsim T_{\nu 0}$ ). Then, if the  $\beta$ -particles are detected with the energy resolution better than  $m_\nu$ , one can tell these two processes apart. Following this observation, various aspects of relic neutrino detection through their capture on beta-decaying nuclei were studied in a number of publications, see e.g. [10–20].

The necessity of separation of the spectra of  $\beta$ -particles produced in relic neutrino capture from those coming from the usual  $\beta$  decay of the target nuclei puts extremely challenging demands on the energy resolution of the detection. Barring the existence of a light predominantly sterile neutrino with a sizeable mixing to the electron flavour and significant presence in  $C\nu B$  and assuming that the neutrino mass spectrum is hierarchical rather than quasi-degenerate, one finds that the energy resolution of at least 0.05 eV is necessary. At present, there is one experimental proposal for relic neutrino detection through their capture on beta-decaying nuclei – the PTOLEMY experiment [21–23], which plans to use tritium as the target. The collaboration has set an ambitious goal of achieving the energy resolution of 0.05 eV for electron detection. It should be noted, however, that in the case of normal neutrino mass ordering (which is currently preferred by the neutrino oscillation data at  $3\sigma$  level [24–26]) and very small mass of the lightest neutrino, even an order of magnitude smaller energy resolution may be necessary [11, 17]. This is related to the fact that in this case the heaviest neutrino with the mass  $m_3 \simeq 0.05$  eV has only a small electron neutrino component  $|U_{e3}|^2 \simeq 2.2 \times 10^{-2}$ . Alternatively, one would need a high enough statistics of the relic neutrino capture events in order to compensate for the smallness of  $|U_{e3}|^2$ .

In the present paper we suggest an alternative method of detecting  $C\nu B$  neutrinos, based on observing *angular correlations* that are characteristic of beta processes. While still exploiting neutrino capture on beta-decaying nuclei, it does not require discrimination between the  $\beta$ -particles coming from relic neutrino capture and from the usual  $\beta$  decay by separating their spectra. Instead, we suggest to employ time variations of the capture rate of relic neutrinos on polarized or unpolarized nuclei arising due to the peculiar motion of the Sun and the rotation of the Earth about its axis.

Neutrino capture on polarized nuclei exhibits several angular correlations, and in particular a correlation between the velocity of the incoming neutrinos and nuclear polarization. Due to the peculiar motion of the solar system with respect to the  $C\nu B$  rest frame, relic neutrinos have a preferred direction of arrival at the Earth. At the same time, if the direction of polarization of the target nuclei is fixed in the Earth-bound lab frame, the angle between this direction and that of the preferred velocity of relic neutrinos varies during the day due to the Earth’s rotation about its axis. One can therefore expect time variation of the relic neutrino signal with the period equal to the sidereal day  $T_0 \simeq 23\text{h } 56\text{m } 4\text{s}$ .<sup>1</sup> No such time variation is expected for the rate of the  $\beta$  decay of the target nuclei.

Relic neutrino capture on polarized nuclei, including possible time variations of the signal due to the peculiar motion of the Sun and the rotation of the Earth, has previously been considered by Lisanti et al. [18] with application to tritium target. However, the authors of [18] discussed this process essentially as a method of obtaining additional information about the properties of  $C\nu B$  neutrinos (such as anisotropies of their velocities and spin distributions) within the usual approach to relic neutrino detection based on the separation of spectra of

---

<sup>1</sup>The sidereal day is the period of the Earth’s rotation about its axis with respect to the distant stars, which is slightly shorter than the solar day because of the Earth’s orbital motion.

electrons from neutrino capture and  $\beta$  decay. By contrast, we focus on using various angular correlations in neutrino capture on polarized nuclear targets as a means of separation of the relic neutrino signal from the background.

We also consider the possibility of using angular correlations for detecting relic neutrinos with unpolarized nuclear targets. This can in principle be done either by measuring polarizations of final-state nuclei or by observing asymmetry of the produced  $\beta$  particles with respect to the preferred direction of relic neutrino arrival at the Earth ( $\beta - \nu$  correlation). The latter should also give rise to a time-dependent signal if the  $\beta$ -asymmetry is studied with respect to a direction that is fixed in the Earth-bound lab frame.

The amplitude of the time variation of the relic neutrino signal is expected to be small, and the problem of reliably detecting this variation in the presence of a large background is very challenging. The main difficulty comes actually not from the high average background level but rather from the fluctuations of the background. Fortunately, there are well-developed methods of such signal-from-noise separation, which are especially efficient when the signal has a known periodicity.

The main advantage of the proposed approach is that it does not depend crucially on the energy resolution of detection of the produced  $\beta$ -particles. While good energy resolution would help to suppress the background from the usual  $\beta$  decay by allowing one to work close to the endpoint of the  $\beta$ -spectrum, the method can still work even if the resolution is relatively large, provided that a sufficiently powerful method of separation of the weak periodic signal from strong random noise is employed. At the same time, the approach based on separation of the spectra will be merely inoperative if the energy resolution of the detection exceeds the largest neutrino mass. One consequence of the fact that the requirements on the energy resolution are less severe in the approach we suggest is that radioactive nuclei with larger  $Q_\beta$  values may be preferable as target, as they lead to larger absolute detection rates.

In our discussion of relic neutrino capture on polarized nuclei we concentrate on pure Gamow-Teller transitions, taking the allowed  $1^\pi \rightarrow 0^\pi$  nuclear transitions as an example. Our results can, however, be readily extended to other Gamow-Teller transitions. One advantage of pure Gamow-Teller transitions is that the effects of target polarization are in general more pronounced in this case. On the other hand, pure Fermi transitions  $0^\pi \rightarrow 0^\pi$  (as well as pure Gamow-Teller ones) may be useful when considering  $\beta - \nu$  angular correlations in relic neutrino capture on unpolarized nuclei. For mixed transitions the correlation coefficient may be strongly suppressed. Another important advantage of pure transitions is that for such transitions the angular correlation coefficients do not depend on nuclear matrix elements.

The paper is organized as follows. In section 2.1 we derive the expression for the differential cross section of neutrino capture on polarized nuclei in the case of allowed Gamow-Teller  $1^\pi \rightarrow 0^\pi$  transitions and discuss various angular correlations relevant to this process. In section 2.2 we consider angular correlations in the case of neutrino capture on unpolarized nuclei. In section 2.3 we compare the results of section 2.1 with those obtained for neutrino capture on polarized tritium [18]. In section 3 we consider effects of averaging over the directions of relic neutrinos on angular correlations in neutrino capture on polarized and unpolarized nuclei observed in the lab frame. In section 4 we discuss the problem of extraction of weak periodic signals from large fluctuating backgrounds and its application to relic neutrino detection. Our results are summarized and discussed in section 5. Appendix A contains some technical details related to the averaging over angular distributions of relic neutrinos. Electron angular asymmetries with respect to fixed directions in the lab frame in experiments with unpolarized targets are considered in Appendix B.

## 2 Neutrino capture in inverse $\beta$ decay

We shall consider neutrino detection in the inverse  $\beta^-$ -decay process

$$\nu_j(q) + A_i(p) \rightarrow A_f(p') + e^-(k), \quad (2.1)$$

where  $\nu_j$  is the  $j$ th neutrino mass eigenstate,  $A_i$  and  $A_f$  are the parent and daughter nuclei, and the 4-momenta of the participating particles are indicated in the parentheses. Detection of relic (anti)neutrino states in inverse  $\beta^+$  decays can be considered quite similarly.

At present,  $C\nu B$  neutrinos originally produced in the states of left-handed chirality should be in left-handed helicity eigenstates in the  $C\nu B$  rest frame, and similarly for the states of right-handed chirality and helicity [17]. Note that, in the Dirac neutrino case, only neutrinos (which are left-helical now) can be captured in the  $\beta^-$ -process (2.1), while right-helical antineutrinos can be detected in inverse  $\beta^+$ -processes. At the same time, if neutrinos are Majorana particles, for non-relativistic neutrinos both left-helical and right-helical states can participate in process (2.1) through their left-chirality components [17].

As helicity is not a Lorentz-invariant quantity, neutrinos that are in helicity eigenstates in some frame  $K$  do not in general have definite helicity in a frame  $K'$  moving with respect to  $K$ . Because the Earth moves with respect to the  $C\nu B$  rest frame, the spins of relic neutrinos need not be aligned or antialigned with their velocities in the lab frame. We therefore consider the differential cross sections of neutrino detection for arbitrary directions of the spins of the initial-state neutrinos.

### 2.1 Gamow-Teller $1^\pi \rightarrow 0^\pi$ transitions

For definiteness, we focus on the allowed  $1^\pi \rightarrow 0^\pi$  Gamow-Teller nuclear transitions, some examples being the decays  $^{32}\text{P} \rightarrow ^{32}\text{S}$ ,  $^{64}\text{Co} \rightarrow ^{64}\text{Ni}$  and  $^{80}\text{Br} \rightarrow ^{80}\text{Kr}$ . We will initially consider the parent nucleus, the incoming neutrino and the produced electron to be in definite spin states, that is, no summation or averaging over their spins is performed. The differential cross section of the process  $d\sigma_j$  multiplied by the neutrino velocity  $v_j$  can then be found as

$$v_j d\sigma_j = \frac{G_\beta^2}{2} |U_{ej}|^2 \frac{1}{(2\pi)^2} \frac{(\varepsilon_\mu \varepsilon_\nu^* X^{\mu\nu})}{4E_e E_j} |M_{\text{GT}}|^2 F(Z, E_e) E_e \sqrt{E_e^2 - m_e^2} d\Omega_e. \quad (2.2)$$

Here  $G_\beta \equiv G_F V_{ud}$ ,  $G_F$  and  $V_{ud}$  being the Fermi constant and the  $ud$  element of the CKM matrix,  $U_{ej}$  are the elements of the leptonic mixing matrix,  $\varepsilon_\mu$  is the polarization 4-vector of the parent nucleus,  $M_{\text{GT}}$  is the nuclear matrix element,  $F(Z, E_e)$  is the Fermi function which takes into account the interaction of the produced electron with the Coulomb field of the daughter nucleus, and  $E_j$  and  $E_e$  are the neutrino and electron energies. Energy conservation yields

$$E_e = E_j + E_0, \quad (2.3)$$

where  $E_0$  is the total energy release in the corresponding  $\beta^-$ -decay process, which is related to the usually quoted  $Q_\beta$ -value of the process in the limit of vanishing neutrino mass by  $E_0 = Q_\beta + m_e$ . The leptonic tensor  $X^{\mu\nu}$  is

$$X^{\mu\nu} = [\bar{u}_e(k) \gamma^\mu (1 - \gamma_5) u_j(q)] [\bar{u}_j(q) \gamma^\nu (1 - \gamma_5) u_e(q)], \quad (2.4)$$

where  $u_e(k)$  is the electron spinor and  $u_j(q)$  is that of the neutrino mass eigenstate with mass  $m_j$ . For electron and neutrino in definite spin states we have

$$u_e(k)\bar{u}_e(k) = \frac{1}{2}(\not{k} + m_e)(1 + \gamma_5 \not{S}_e), \quad (2.5)$$

$$u_j(q)\bar{u}_j(q) = \frac{1}{2}(\not{q} + m_j)(1 + \gamma_5 \not{S}_j), \quad (2.6)$$

where  $m_e$  and  $m_j$  are the electron and neutrino masses, and  $S_e^\mu$  and  $S_j^\mu$  are their spin 4-vectors:

$$S_e^\mu = \left( \frac{\vec{k} \cdot \vec{s}_e}{m_e}, \vec{s}_e + \frac{(\vec{k} \cdot \vec{s}_e)\vec{k}}{m_e(E_e + m_e)} \right), \quad (2.7)$$

$$S_j^\mu = \left( \frac{\vec{q} \cdot \vec{s}_j}{m_j}, \vec{s}_j + \frac{(\vec{q} \cdot \vec{s}_j)\vec{q}}{m_j(E_j + m_j)} \right). \quad (2.8)$$

Here  $\vec{s}_e$  and  $\vec{s}_j$  are, respectively, the unit vectors in the direction of the electron and neutrino spin in their rest frames. Introducing the 4-vectors

$$A^\mu \equiv k^\mu - m_e S_e^\mu, \quad B^\mu \equiv q^\mu - m_j S_j^\mu, \quad (2.9)$$

we can write the squared amplitude  $\varepsilon_\mu \varepsilon_\nu^* X^{\mu\nu}$  in a very compact form:<sup>2</sup>

$$\varepsilon_\mu \varepsilon_\nu^* X^{\mu\nu} = 2(A^0 - \vec{A} \cdot \vec{s}_N)(B^0 + \vec{B} \cdot \vec{s}_N). \quad (2.10)$$

Here  $\vec{s}_N$  is the unit vector in the direction of the spin of the initial-state nucleus. Defining

$$K_e \equiv 1 - \frac{E_e}{E_e + m_e} \vec{v}_e \cdot \vec{s}_e, \quad K_j \equiv 1 - \frac{E_j}{E_j + m_j} \vec{v}_j \cdot \vec{s}_j, \quad (2.11)$$

we can rewrite  $A^\mu$  and  $B^\mu$  as

$$A^\mu = E_e \left( 1 - \vec{v}_e \cdot \vec{s}_e, K_e \vec{v}_e - \frac{m_e}{E_e} \vec{s}_e \right), \quad (2.12)$$

$$B^\mu = E_j \left( 1 - \vec{v}_j \cdot \vec{s}_j, K_j \vec{v}_j - \frac{m_j}{E_j} \vec{s}_j \right). \quad (2.13)$$

Substituting these expressions into eq. (2.10), we find

$$\begin{aligned} \varepsilon_\mu \varepsilon_\nu^* X^{\mu\nu} &= 2E_e E_j \left[ (1 - \vec{v}_e \cdot \vec{s}_e) - K_e (\vec{v}_e \cdot \vec{s}_N) + \frac{m_e}{E_e} (\vec{s}_e \cdot \vec{s}_N) \right] \\ &\quad \times \left[ (1 - \vec{v}_j \cdot \vec{s}_j) + K_j (\vec{v}_j \cdot \vec{s}_N) - \frac{m_j}{E_j} (\vec{s}_j \cdot \vec{s}_N) \right]. \end{aligned} \quad (2.14)$$

The above expressions give the differential cross section of neutrino capture on polarized nuclei (in the particular case of allowed  $1^\pi \rightarrow 0^\pi$  Gamow-Teller transitions) without summation over the spin states of any of the involved particles or integration over the directions of

---

<sup>2</sup> Note that, since the electron and neutrino spin 4-vectors satisfy the usual relations  $k \cdot S_e = q \cdot S_j = 0$  and  $S_e^2 = S_j^2 = -1$ , the 4-vectors  $A^\mu$  and  $B^\mu$  are lightlike:  $A^2 = B^2 = 0$ . When the vector  $\vec{s}_j$  is aligned or antialigned with  $\vec{s}_N$ , for neutrinos that are in helicity eigenstates the vector  $\vec{B}$  is also aligned or antialigned with  $\vec{s}_N$ . In this case from  $B^2 = 0$  it follows that  $\vec{B} \cdot \vec{s}_N = \pm B^0$ . For  $\vec{s}_j \parallel \vec{s}_N$  we find  $\vec{B} \cdot \vec{s}_N = -B^0$ , and the transition amplitude vanishes. One can similarly show that it also vanishes when the emitted electron is in a helicity eigenstate and its spin is antialigned with  $\vec{s}_N$  (see also section 5 below).

their momenta. To our knowledge, no such expression has been previously derived. When the summations over the spin states of the neutrino and the electron, or of the neutrino and the parent nucleus, or the summation over the neutrino spin states and integration over the direction of its momentum are performed, our results coincide with the corresponding results found by Jackson et al. [27, 28].

The amplitude of the process under consideration depends on five vectors –  $\vec{v}_e$ ,  $\vec{v}_j$ ,  $\vec{s}_e$ ,  $\vec{s}_j$  and  $\vec{s}_N$ , from which one can form ten scalar dot-products:

$$\begin{aligned} & \vec{v}_e \cdot \vec{s}_e, \quad \vec{v}_e \cdot \vec{s}_N, \quad \vec{s}_e \cdot \vec{s}_N, \quad \vec{v}_j \cdot \vec{s}_j, \\ & \vec{v}_e \cdot \vec{v}_j, \quad \vec{v}_e \cdot \vec{s}_j, \quad \vec{v}_j \cdot \vec{s}_e, \quad \vec{s}_e \cdot \vec{s}_j, \quad \vec{v}_j \cdot \vec{s}_N, \quad \vec{s}_j \cdot \vec{s}_N. \end{aligned} \quad (2.15)$$

Eq. (2.14) actually contains only on six of them: terms containing the quantities  $\vec{v}_e \cdot \vec{v}_j$ ,  $\vec{v}_e \cdot \vec{s}_j$ ,  $\vec{v}_j \cdot \vec{s}_e$  and  $\vec{s}_e \cdot \vec{s}_j$  are absent from the squared amplitude of the process. They will, however, arise if one averages over the directions of nuclear polarization  $\vec{s}_N$ , i.e. considers neutrino capture on unpolarized nuclei (see eqs. (2.17)-(2.20) in section 2.2 below).

Out of the ten scalar dot-products in eq. (2.15), those in the first line are not useful for discriminating between neutrino capture and neutrino emission in  $\beta$  decay. Indeed, the first three of them do not depend on the neutrino variables, whereas the last one,  $\vec{v}_j \cdot \vec{s}_j$ , is not helpful because experiments on neutrino helicity measurements cannot distinguish between absorption of a left-helical neutrino and production of a right-helical (anti)neutrino. The term  $\vec{v}_j \cdot \vec{s}_j$ , however, affects the total neutrino capture rate and may also play an important role in studying Dirac vs. Majorana neutrino nature in captures of relic neutrinos (see [17, 19] and section 3 below).

Out of the six scalars in the second line of (2.15), only the last two enter into the squared amplitude in eq. (2.14). They result in angular correlations between the nuclear polarization and the directions of neutrino spin and velocity. Summing eq. (2.14) over the electron spin states and averaging over the directions of the produced electrons, we find

$$\int \frac{d\Omega_e}{4\pi} \sum_{s_e} \varepsilon_\mu \varepsilon_\nu^* X^{\mu\nu} = 4E_e E_j \left\{ (1 - \vec{v}_j \cdot \vec{s}_j) + \left( K_j \vec{v}_j - \frac{m_j}{E_j} \vec{s}_j \right) \cdot \vec{s}_N \right\}. \quad (2.16)$$

If the direction of nuclear polarization is fixed in the Earth frame, this squared amplitude will vary with time because of variations of the directions of the spin and velocity of the incoming neutrinos. Therefore, in experiments with polarized nuclear targets one can study time variations of the relic neutrino signal by merely measuring the total rate of electron production. At the same time, as we shall see in section 2.2, measuring the angular and/or spin distributions of the produced electrons will be useful in the case of experiments with unpolarized nuclei.

In order to derive the expressions for the total capture rate of the  $C\nu B$  neutrinos as well as for various angular correlations of interest, one has to multiply eq. (2.2) by the neutrino velocity distribution function of the  $j$ th neutrino mass-eigenstate  $f(\vec{v}_j)$ , integrate or sum over the relevant finite-state kinematic variables and sum the result over  $j$ .

## 2.2 Neutrino capture on unpolarized nuclei

Polarizing sufficiently large targets and maintaining (or renewing) their polarization during extended intervals of time may pose substantial experimental difficulties. Can angular correlations help discriminate between relic neutrino capture and  $\beta$  decay of the target nuclei in experiments with unpolarized targets? One possibility is to make use of spin polarization of

the daughter nuclei with  $J \neq 0$ . This polarization can be studied, for instance, by measuring circular polarization of the de-excitation  $\gamma$ -quanta in  $\beta$ -transitions into excited states of the daughter nuclei, as in the famous experiment of Goldhaber, Grodzins and Sunyar [29]. For the particular case of the allowed Gamow-Teller  $0^\pi \rightarrow 1^\pi$  transitions, the corresponding squared amplitude can be obtained from the expressions in eqs. (2.10) or (2.14) by the substitution  $\vec{s}_N \rightarrow -\vec{s}_N$  (assuming that the velocity of the recoil nucleus can be neglected).

Another, probably more practical, possibility is to study angular distributions of the produced electrons or their spin states. For neutrino capture on unpolarized nuclei in allowed Gamow-Teller  $1^\pi \rightarrow 0^\pi$  transitions the squared amplitude can be found by averaging  $\varepsilon_\mu \varepsilon_\nu^* X^{\mu\nu}$  over the polarizations  $\lambda$  of the parent nucleus. Direct calculation gives

$$\frac{1}{3} \sum_{\lambda} \varepsilon_\mu(\lambda) \varepsilon_\nu^*(\lambda) X^{\mu\nu} = 2 \left[ A^0 B^0 - \frac{1}{3} \vec{A} \cdot \vec{B} \right]. \quad (2.17)$$

Note that the same result can be obtained by averaging eq. (2.10) over the directions of  $\vec{s}_N$  (i.e. by taking  $\int (d\Omega_{\vec{s}_N}/4\pi)$  of both its parts). Let us first consider the case when the spin state of the produced electron is not measured. Summing eq. (2.17) over  $s_e$ , we find

$$\frac{1}{3} \sum_{\lambda, s_e} \varepsilon_\mu(\lambda) \varepsilon_\nu^*(\lambda) X^{\mu\nu} = 4E_e \left( B^0 - \frac{1}{3} \vec{B} \cdot \vec{v}_e \right), \quad (2.18)$$

or, in a more detailed form,

$$\frac{1}{3} \sum_{\lambda, s_e} \varepsilon_\mu(\lambda) \varepsilon_\nu^*(\lambda) X^{\mu\nu} = 4E_e E_j \left[ 1 - \vec{v}_j \cdot \vec{s}_j - \frac{1}{3} \vec{v}_e \cdot \vec{v}_j + \frac{1}{3} \frac{E_j}{E_j + m_j} (\vec{v}_j \cdot \vec{s}_j) (\vec{v}_e \cdot \vec{v}_j) + \frac{1}{3} \frac{m_j}{E_j} \vec{v}_e \cdot \vec{s}_j \right]. \quad (2.19)$$

Alternatively, one can consider the situation when the direction of the spin of the produced electrons is observed, while the directions of their momenta are not. Then the relevant squared amplitude is

$$\begin{aligned} \int \frac{d\Omega_e}{4\pi} \frac{1}{3} \sum_{\lambda} \varepsilon_\mu(\lambda) \varepsilon_\nu^*(\lambda) X^{\mu\nu} &= 2E_e \left\{ B^0 + \frac{1}{9} \left( 1 + 2 \frac{m_e}{E_e} \right) (\vec{s}_e \cdot \vec{B}) \right\} \\ &= 2E_e E_j \left\{ 1 - \vec{v}_j \cdot \vec{s}_j + \frac{1}{9} \left( 1 + 2 \frac{m_e}{E_e} \right) \left[ \vec{v}_j \cdot \vec{s}_e - \frac{E_j}{E_j + m_j} (\vec{v}_j \cdot \vec{s}_j) (\vec{v}_j \cdot \vec{s}_e) - \frac{m_j}{E_j} \vec{s}_e \cdot \vec{s}_j \right] \right\}. \end{aligned} \quad (2.20)$$

Eq. (2.19) describes anisotropies of electron emission with respect to the directions of the velocity and spin of the incoming relic neutrinos  $\vec{v}_j$  and  $\vec{s}_j$ , which change with time in the lab frame. The electron direction anisotropy with respect to a fixed direction in this frame should therefore exhibit time variations. The same applies to the electron spin anisotropy described by eq. (2.20). This in principle could be used to find out the direction of the peculiar motion of the Sun with respect to the  $C\nu B$  rest frame.

In the case when neither the spin state nor the direction of the produced electron is observed, the relevant squared amplitude is

$$\int \frac{d\Omega_e}{4\pi} \frac{1}{3} \sum_{\lambda, s_e} \varepsilon_\mu(\lambda) \varepsilon_\nu^*(\lambda) X^{\mu\nu} = 4E_e E_j (1 - \vec{v}_j \cdot \vec{s}_j), \quad (2.21)$$

which is the usual inclusive squared amplitude for neutrino capture on unpolarized nuclei.



### 2.3 Comparison with $\nu$ capture on polarized tritium ( $1/2^+ \rightarrow 1/2^+$ )

It is instructive to compare our results obtained for pure Gamow-Teller  $1^\pi \rightarrow 0^\pi$  transitions with those found by Lisanti et al. for neutrino capture on polarized tritium, which is the mixed Fermi–Gamow-Teller  $1/2^+ \rightarrow 1/2^+$  transition [18]. The authors calculated the squared amplitude in the case when the spin states of the produced electron and daughter  $^3\text{He}$  are not measured and found the angular correlation (in our notation)

$$1 - \vec{v}_j \cdot \vec{s}_j + A(1 - \vec{v}_j \cdot \vec{s}_j)\vec{v}_e \cdot \vec{s}_N + BK_j\vec{v}_j \cdot \vec{s}_N - B\frac{m_j}{E_j}\vec{s}_j \cdot \vec{s}_N + aK_j\vec{v}_e \cdot \vec{v}_j - a\frac{m_j}{E_j}\vec{v}_e \cdot \vec{s}_j. \quad (2.22)$$

Here  $A$ ,  $B$  and  $a$  are the standard angular correlation coefficients [27, 28], which can be expressed through the ratios of the Fermi and Gamow-Teller nuclear matrix elements  $M_F$  and  $M_{GT}$ . For the considered case of neutrino capture on polarized tritium their numerical values are [18]

$$A \simeq -0.095, \quad B \simeq 0.99, \quad a \simeq -0.087. \quad (2.23)$$

To compare eq. (2.22) with our results, one has to sum our squared amplitude (2.14) over  $s_e$ . The obtained angular correlation is

$$1 - \vec{v}_j \cdot \vec{s}_j - (1 - \vec{v}_j \cdot \vec{s}_j)\vec{v}_e \cdot \vec{s}_N + K_j\vec{v}_j \cdot \vec{s}_N - \frac{m_j}{E_j}\vec{s}_j \cdot \vec{s}_N - K_j(\vec{v}_j \cdot \vec{s}_N)(\vec{v}_e \cdot \vec{s}_N) + \frac{m_j}{E_j}(\vec{v}_e \cdot \vec{s}_N)(\vec{s}_j \cdot \vec{s}_N). \quad (2.24)$$

One can see that the first five terms in eq. (2.22) have the same structure as the first five terms in eq. (2.24); the two sets coincide with each other if one chooses  $A = -1$  and  $B = 1$  in (2.22). At the same time, the last two terms in (2.22), which have the coefficient  $a$  as a factor, are different from the last two terms in (2.24). The latter are bilinear in the polarization vector of the parent nucleus  $\vec{s}_N$ , while eq. (2.22) contains only terms of zero and first power in  $\vec{s}_N$ . The origin of this difference in the structures of eqs. (2.22) and (2.24) lies in the special nature of the  $1/2^+ \rightarrow 1/2^+$  transition, for which the tensor alignment  $\propto [J(J+1) - 3(\vec{J} \cdot \vec{s}_N)^2]$  vanishes [27]. It is interesting to note that upon averaging over the directions of  $\vec{s}_N$  the last two terms in eq. (2.24) would reproduce those in eq. (2.22) with  $a = -1/3$ .

Although effects of angular correlations are in general more prominent in the case of pure Gamow-Teller transitions than in the case of mixed Fermi–Gamow-Teller ones, the correlation between the velocity (and/or spin) of the incoming neutrino and nuclear polarization in neutrino capture on polarized tritium is quite substantial. This follows from the fact that the coefficient  $B$  governing these correlations is close to unity (see eq. (2.23)). At the same time, the  $\beta - \nu$  correlation, which exists even for processes on unpolarized nuclei, is suppressed in this transition due to the numerical smallness of the coefficient  $a$ . By contrast, this coefficient is significant in the case of pure transitions:  $a = -1/3$  for pure Gamow-Teller allowed transitions and  $a = 1$  for pure Fermi allowed or superallowed transitions  $0^\pi \rightarrow 0^\pi$ .

### 3 Implications for relic neutrino capture: lab frame

Standard cosmology predicts the existence of a background of nearly uniform and isotropic cosmic neutrinos with the average density of  $n_{\nu 0} \simeq 56 \text{ cm}^{-3}$  per mass eigenstate and per spin degree of freedom. Relic neutrinos are expected to be in helicity eigenstates in the  $C\nu B$  rest frame, and therefore not only their velocities, but also their spin directions should be distributed isotropically in that frame. As at least two relic neutrino species should now be

non-relativistic, gravitational clustering may modify the local density of CνB at the Earth’s location (see, e.g., [30] and references therein). Gravitational focusing by the Sun can also modify local neutrino density and velocity distribution, leading to annual modulations of the relic neutrino signal at the Earth [16]. These effects are, however, expected to be relatively small in the case of hierarchical neutrino mass spectrum and will not be discussed here.

The Sun is expected to have a non-zero peculiar velocity with respect to the CνB rest frame, therefore there should exist a “wind” of relic neutrinos at the Earth, i.e. they should have a preferred direction of arrival in the Earth’s rest frame. Although the speed and the direction of the peculiar motion of the Sun are model-dependent and thus not precisely known, it is expected that the peculiar velocity  $u$  is rather small,  $\mathcal{O}(10^{-3})$ . The daily rotation of the Earth about its axis means that direction of the neutrino “wind” changes during the day in the lab frame, which should lead to modulations of various angular correlations in relic neutrino capture on both polarized and unpolarized nuclei. Our goal is to study if these modulations can be used to distinguish neutrino capture from the usual  $\beta$ -decay of target nuclei. Our discussion of the effects of anisotropy of relic neutrinos will differ from that in ref. [18] in two important respects:

- While the authors of [18] concentrated on non-relativistic relic neutrinos, we consider the general case, since in the case of the normal neutrino mass ordering currently preferred by the data the lightest neutrino mass eigenstate  $\nu_1$  (which has the largest contribution of the electron flavour  $|U_{e1}|^2 \simeq 0.66$ ) may still be relativistic.
- We consider angular correlations in neutrino captures on both polarized and unpolarized nuclear targets. In particular, the  $\beta - \nu$  angular correlation can be quite sizeable for unpolarized pure Gamow-Teller or pure Fermi transitions though it is suppressed for the mixed Fermi–Gamow-Teller one studied in [18].

We want to find the neutrino differential capture rate in an Earth-bound lab frame which moves with respect to the CνB rest frame with the velocity  $-\vec{u}$  with  $u \equiv |\vec{u}| \ll 1$ . To this end, we consider the effects of the Lorentz boost on the neutrino variables to first order in the boost velocity  $u$ . Let us denote neutrino variables in the lab frame with primed quantities, whereas the unprimed variables will refer to the CνB rest frame. For the energy, momentum and velocity of the  $j$ th neutrino mass eigenstate in the lab frame we then have

$$E'_j = E_j + \vec{u} \cdot \vec{q}, \quad \vec{q}' = \vec{q} + \vec{u} E_j, \quad \vec{v}'_j = \vec{v}_j (1 - \vec{u} \cdot \vec{v}_j) + \vec{u}. \quad (3.1)$$

We will be mostly interested in the regime  $u \ll v_j$ , which in the standard 3-flavour neutrino picture corresponds to hierarchical neutrino mass spectrum with the largest neutrino mass of order 0.05 eV. In this limit for the unit vector in the direction of the neutrino velocity in the Earth frame we find

$$\frac{\vec{v}'_j}{v'_j} = \frac{1}{v_j} \left\{ \vec{v}_j + \left[ \vec{u} - \frac{(\vec{u} \cdot \vec{v}_j)}{v_j^2} \vec{v}_j \right] \right\} \equiv \frac{1}{v_j} (\vec{v}_j + \vec{u}_{\perp j}), \quad (3.2)$$

where  $\vec{u}_{\perp j}$  is the component of the boost velocity  $\vec{u}$  orthogonal to  $\vec{v}_j$ .

The neutrino spin requires a special consideration. The spin 4-vector  $S_j^\mu$  in eq. (2.8) can be obtained from the rest-frame vector  $S_j^{(0)\mu} = (0, \vec{s}_j)$  by a Lorentz boost. The corresponding 4-vector in the Earth frame,  $S_j^{\prime\mu}$ , is then obtained by another boost, with velocity  $\vec{u}$ . The

result will have the form similar to that in eq. (2.8), with all the quantities in it replaced by the primed ones. Note that in general  $\vec{s}'_j \neq \vec{s}_j$ ; this is related to the fact that a sequence of two boosts with non-collinear velocities is equivalent to a boost and a rotation (called the Wigner rotation) rather than to a single boost. The general expression for  $\vec{s}'_j$  is rather involved, but to first order in  $u$  one finds a simple result<sup>3</sup>

$$\vec{s}'_j = \vec{s}_j + \frac{(\vec{q} \cdot \vec{s}_j)\vec{u} - (\vec{u} \cdot \vec{s}_j)\vec{q}}{E_j + m_j}. \quad (3.3)$$

Assume now that in the  $C\nu B$  rest frame neutrinos are in the exact helicity eigenstates, i.e.

$$\vec{s}_j = \lambda_j \frac{\vec{v}_j}{v_j}, \quad (3.4)$$

where  $\lambda_j = \pm 1$ , with the upper (lower) sign corresponding to right-helical (left-helical) neutrinos. Then

$$\vec{s}'_j = \lambda_j \left\{ \frac{\vec{v}_j}{v_j} + v_j \frac{E_j}{E_j + m_j} \vec{u}_{\perp j} \right\}. \quad (3.5)$$

It is interesting to note that, even though helicity is not a Lorentz-invariant quantity, in the regime  $u \ll v_j$  of main interest to us and to first order in the boost velocity  $u$  the neutrino helicity in the lab frame is the same as in the  $C\nu B$  rest frame. This follows from the fact that for small boosts the correction to  $\vec{s}_j$  (i.e. the second term in the curly brackets in eq. (3.5)) is of order  $u$  and orthogonal to  $\vec{v}_j$ , and in the limit  $u \ll v_j$  the correction to the unit vector of the neutrino velocity in eq. (3.2) is orthogonal to  $\vec{s}_j$ , which is collinear with  $\vec{v}_j$ . Therefore, the correction to  $\vec{s}_j \cdot \vec{v}_j/v_j$  is quadratic in  $u$  in this limit and can be neglected.<sup>4</sup>

Next, we will consider the consequences of the fact that  $C\nu B$  is isotropic in its rest frame for the average characteristics of relic neutrinos in the lab frame. In the  $C\nu B$  rest frame we have  $\langle \vec{v}_j \rangle = 0$ ,  $\langle \vec{s}_j \rangle = 0$  (hereafter the angular brackets will denote averaging over the angular distributions of the  $C\nu B$  neutrinos but not over the absolute values of the neutrino velocities  $v_j$ ). Therefore, for the quantities in the lab frame we get

$$\langle E'_j \rangle = E_j, \quad \langle \vec{q}' \rangle = \vec{u} E_j, \quad \langle \vec{v}'_j \rangle = \left( 1 - \frac{v_j^2}{3} \right) \vec{u}. \quad (3.6)$$

Further discussion of the effects of averaging over the directions of  $C\nu B$  neutrinos on neutrino observables in the lab frame can be found in Appendix A.

### 3.1 Polarized targets

Let us consider now  $C\nu B$  detection by capture on polarized targets in the lab frame. For the squared amplitude of the allowed  $1^\pi \rightarrow 0^\pi$  transition one finds (see Appendix A)

$$\left\langle \frac{\varepsilon_\mu \varepsilon_\nu^* X^{\mu\nu}}{4E_e E'_j} \right\rangle = \frac{1}{2E_e} (A^0 - \vec{A} \cdot \vec{s}_N) \left\{ 1 - \lambda_j v_j + \left( 1 - \frac{2}{3} \lambda_j v_j - \frac{v_j^2}{3} \right) \vec{u} \cdot \vec{s}_N \right\}. \quad (3.7)$$

<sup>3</sup>It can be readily obtained by applying the Lorentz boost to linear order in the boost velocity  $\vec{u}$  to the 4-vector  $S_j^\mu$  and requiring that in the primed variables it have the same form as eq. (2.8).

<sup>4</sup>Note that this would not be in general correct for  $u \gtrsim v_j$  (which corresponds to neutrino mass  $m_j \gtrsim 0.5$  eV), even if  $u$  is small. In particular, for  $v_j \ll u \ll 1$  we would have  $\vec{v}'_j \simeq \vec{u}$ ,  $\vec{s}'_j \simeq \vec{s}_j$  and  $\vec{s}'_j \cdot \vec{v}'_j/v'_j \simeq \vec{s}_j \cdot \vec{u}/u$ , which is different from  $\lambda_j$  for all boost velocities  $\vec{u}$  that are not parallel or antiparallel to  $\vec{v}_j$ .

The part of this expression relevant to our discussion is the last factor on the right hand side. As the direction of  $\vec{u}$  in the lab frame changes during the day because of the rotation of the Earth, this factor gives rise to periodic variations of the signal, provided that the nuclear polarization vector  $\vec{s}_N$  is not oriented along the Earth's rotation axis. The amplitude of the time variations is maximal when  $\vec{s}_N$  is orthogonal to this axis.<sup>5</sup> Let us now examine the effects of these time-dependent angular correlations.

Let  $\mathcal{F}_j(\lambda_j)$  denote the expression in the curly brackets in eq. (3.7). For left-helical neutrinos we have

$$\mathcal{F}_j(\lambda_j = -1) = 1 + v_j + \left(1 + \frac{2}{3}v_j - \frac{v_j^2}{3}\right)\vec{u}\cdot\vec{s}_N. \quad (3.8)$$

For right-helical neutrino states we have to distinguish between Dirac and Majorana neutrinos. In the Dirac case, right-helical states are antineutrinos which cannot be detected in inverse  $\beta^-$ -decay processes, that is, one has to set  $\mathcal{F}_j(\lambda_j = 1) = 0$  in that case. For Majorana neutrinos we have

$$\mathcal{F}_j(\lambda_j = 1) = 1 - v_j + \left(1 - \frac{2}{3}v_j - \frac{v_j^2}{3}\right)\vec{u}\cdot\vec{s}_N. \quad (3.9)$$

In the limit  $v_j \rightarrow 1$  this expression vanishes, in accord with the fact that ultra-relativistic Dirac and Majorana neutrinos are essentially indistinguishable.

Assuming that C $\nu$ B contains equal numbers of left-helical and right-helical neutrinos and summing over the helicities, we find

$$\mathcal{F}_j \equiv \sum_{\lambda_j=\pm 1} \mathcal{F}_j(\lambda_j) = \begin{cases} 1 + v_j + \left(1 + \frac{2}{3}v_j - \frac{v_j^2}{3}\right)\vec{u}\cdot\vec{s}_N, & \text{Dirac neutrinos,} \\ 2\left[1 + \left(1 - \frac{v_j^2}{3}\right)\vec{u}\cdot\vec{s}_N\right], & \text{Majorana neutrinos.} \end{cases} \quad (3.10)$$

In the limiting case of non-relativistic neutrinos this gives

$$\mathcal{F}_j \simeq \begin{cases} 1 + v_j + \left(1 + \frac{2}{3}v_j\right)\vec{u}\cdot\vec{s}_N, & \text{Dirac neutrinos,} \\ 2\left(1 + \vec{u}\cdot\vec{s}_N\right), & \text{Majorana neutrinos.} \end{cases} \quad (3.11)$$

For highly relativistic neutrinos we obtain

$$\mathcal{F}_j^{Dir} \simeq \mathcal{F}_j^{Maj} \simeq 2\left(1 + \frac{2}{3}\vec{u}\cdot\vec{s}_N\right). \quad (3.12)$$

Let us consider more closely the regime of non-relativistic neutrinos, in which the results for Dirac and Majorana neutrinos differ. Dropping in (3.11) the term proportional to  $\vec{u}\cdot\vec{s}_N$ , we recover the result of [17] obtained for neutrino absorption by unpolarized nuclei: the detection cross section for Majorana neutrinos is about twice as large as that for Dirac neutrinos, which means that detection of relic neutrinos could in principle shed light on neutrino nature. This is, however, complicated by the fact that the local C $\nu$ B density at the Earth may differ from  $n_{\nu 0}$  due to gravitational clustering effects and so is not precisely known. Because the detection rate of relic neutrinos is proportional to their local density, by measuring only the absolute C $\nu$ B detection rate one may not be able to determine neutrino nature unambiguously.

---

<sup>5</sup>In the geocentric spherical coordinates we have  $\vec{u}\cdot\vec{s}_N = u[\cos\theta_u \cos\theta_N + \sin\theta_u \sin\theta_N \cos(\phi_u(t) - \phi_N)]$  with  $\phi_u(t) = (2\pi/T_0)t + \phi_0$ ,  $T_0$  being the sidereal day. As the declination  $\theta_u$  of the vector  $\vec{u}$  is fixed, the time dependence of  $\vec{u}\cdot\vec{s}_N$  is maximized when  $\sin\theta_N = 1$ , i.e. when  $\vec{s}_N$  is orthogonal to the Earth's rotation axis.

As can be seen from eq. (3.11), this degeneracy between unknown local relic neutrino density and Dirac/Majorana neutrino nature can in principle be lifted by measuring time-dependent angular correlations in relic neutrino capture. This follows from the difference of the dependences of  $\mathcal{F}_j$  on  $\vec{u} \cdot \vec{s}_N$  in the Dirac and Majorana cases, which cannot be absorbed in the overall normalization of  $\mathcal{F}_j$ . In practice, however, making use of this difference will be very difficult because it contains an extra factor  $v_j$  compared to the main  $\vec{u} \cdot \vec{s}_N$  term.

### 3.2 Unpolarized targets

Let us now turn to angular correlations in the case of relic neutrino capture on unpolarized targets. By averaging eq. (3.7) over the polarizations of the parent nuclei we find

$$\left\langle \frac{1}{3} \sum_{\lambda} \frac{\varepsilon_{\mu}(\lambda) \varepsilon_{\nu}^*(\lambda) X^{\mu\nu}}{4E_e E'_j} \right\rangle = \frac{1}{2E_e} \left\{ A^0 (1 - \lambda_j v_j) - \frac{1}{3} \left( 1 - \frac{2}{3} \lambda_j v_j - \frac{v_j^2}{3} \right) \vec{u} \cdot \vec{A} \right\}. \quad (3.13)$$

Consider this expression in two special cases. If the spin state of the produced electron is not measured, summing over  $s_e$  we obtain

$$\left\langle \frac{1}{3} \sum_{\lambda, s_e} \frac{\varepsilon_{\mu}(\lambda) \varepsilon_{\nu}^*(\lambda) X^{\mu\nu}}{4E_e E'_j} \right\rangle = 1 - \lambda_j v_j - \frac{1}{3} \left( 1 - \frac{2}{3} \lambda_j v_j - \frac{v_j^2}{3} \right) \vec{u} \cdot \vec{v}_e. \quad (3.14)$$

If the electron direction is not observed but its spin state is, we find

$$\int \frac{d\Omega_e}{4\pi} \left\langle \frac{1}{3} \sum_{\lambda} \frac{\varepsilon_{\mu}(\lambda) \varepsilon_{\nu}^*(\lambda) X^{\mu\nu}}{4E_e E'_j} \right\rangle = \frac{1}{2} \left\{ 1 - \lambda_j v_j + \frac{1}{9} \left( 1 + 2 \frac{m_e}{E_e} \right) \left( 1 - \frac{2}{3} \lambda_j v_j - \frac{v_j^2}{3} \right) \vec{u} \cdot \vec{s}_e \right\}. \quad (3.15)$$

Through the terms proportional to  $\vec{u} \cdot \vec{v}_e$  and  $\vec{u} \cdot \vec{s}_e$ , these expressions exhibit angular correlations between the directions of the electron's velocity or spin and the preferred direction of relic neutrino arrival  $\vec{u}$  which changes in the lab frame during the day. Therefore, the probability of electron emission with its momentum (or spin) pointing in a certain direction in the lab frame will in general exhibit periodic time variations. The variations are absent for the directions collinear with the Earth's rotation axis and are maximized for the orthogonal directions (see Appendix B).

Note that the right hand side of eq. (3.14) can be formally obtained from  $\mathcal{F}_j(\lambda_j)$  by the replacement  $\vec{u} \cdot \vec{s}_N \rightarrow (-1/3)\vec{u} \cdot \vec{v}_e$ , and similarly that of eq. (3.15) is obtained from  $\mathcal{F}_j(\lambda_j)$  by replacing  $\vec{u} \cdot \vec{s}_N \rightarrow (1/9)[1 + 2(m_e/E_e)]\vec{u} \cdot \vec{s}_e$  and multiplying the whole expression by 1/2. Therefore, the discussion of the summation over the neutrino helicities, non-relativistic and ultra-relativistic neutrino limits and the differences between the Dirac and Majorana neutrino detection rates in the unpolarized case is quite similar to that for neutrino capture on polarized targets in section 3.1 and will not be repeated here.

## 4 Separation of periodic signal from large fluctuating background

The amplitude of periodic variations of the angular correlations in relic neutrino captures on beta-decaying nuclei is expected to be only a small ( $\sim 0.1\%$ ) fraction of the signal itself. In addition, except in the case of very high energy resolution, the overall relic neutrino signal is going to be very small compared with the background coming from the usual  $\beta$  decay of the target nuclei. Indeed, the ratio of neutrino capture rate to the rate of the competing  $\beta$

decay with production of electrons in the energy window  $\delta$  just below the endpoint of the  $\beta$ -spectrum is [9, 10]

$$\frac{\Gamma_c}{\Gamma_d} \simeq 6\pi^2 \frac{n_\nu}{\delta^3} \simeq \frac{n_\nu}{56 \text{ cm}^{-3}} \frac{2.54 \times 10^{-11}}{[\delta \text{ (eV)}]^3}, \quad (4.1)$$

independently of the  $Q_\beta$ -value of the process. Thus, e.g., for  $n_\nu = 56 \text{ cm}^{-3}$  and  $\delta = 0.1 \text{ eV}$  the ratio is about  $2.5 \times 10^{-8}$ . Clearly, in looking for the time dependence of the relic neutrino signal one would face a very difficult task of extracting a weak periodic signal from large fluctuating backgrounds.

The problem of separation of signals from noisy backgrounds is actually well studied. It is routinely encountered in astronomy, acoustics, radiodetection, engineering, medical applications such as electrocardiography, magnetic resonance imaging, etc. There exists an enormous literature on the subject. Here we shall consider a simple approach to signal-from-noise separation based on the Fourier analysis and filtering in the frequency domain.

We are interested in observing small periodic variations of the detection rate of electrons produced in neutrino capture on polarized nuclei in the presence of a large background of electrons coming from the usual  $\beta$  decay and possibly from other background sources. We also include in our definition of the background a (small) contribution coming from the average neutrino capture rate. The periodic component of the signal is thus defined to have zero time average. The background will be considered to be time-independent, except for the usual statistical fluctuations due to the quantum nature of the underlying processes.<sup>6</sup>

In extracting periodic signals from large backgrounds the main problem comes from the fluctuations of the background rather than from its average. We therefore subtract the mean rate of the background events from the overall signal and consider

$$f(t) = s(t) + n(t), \quad (4.2)$$

where  $s(t)$  is the periodic signal and the  $n(t)$  is the “noise” which represents statistical fluctuations of the background. This is actually the form usually considered in the signal processing theory. Since by their definition both the signal  $s(t)$  and the noise  $n(t)$  have zero time averages, their strengths are characterized by their variances,  $\overline{s(t)^2}$  and  $\overline{n^2(t)}$ .

In our treatment we will consider the periodic signal of the sinusoidal form

$$s(t) = A_0 \sin(\omega_0 t + \varphi) \quad (4.3)$$

with the period  $T_0 = 2\pi/\omega_0$  and constant amplitude  $A_0$  and phase  $\varphi$ .<sup>7</sup> The statistical properties of signal and noise are usually described in the time domain by their autocorrelation functions,  $R_{ss}(\tau)$  and  $R_{nn}(\tau)$ , and in the frequency domain by their power spectra [31–36]. Let us first consider the limit of infinite total observation time  $T$  and infinite measurement bandwidth. The autocorrelation function for the signal is defined as

$$R_{ss}(\tau) = \overline{s(t)s(t+\tau)} \equiv \lim_{T \rightarrow \infty} \frac{1}{T} \int_{-T/2}^{T/2} s(t)s(t+\tau) dt, \quad (4.4)$$

---

<sup>6</sup> For large overall observation time  $T$  comparable to the mean lifetime of the target nuclei one should take into account the exponential decrease with time of both the amplitude of the periodic signal and the background. In this case the mean background to be subtracted from the signal in order to ensure that it has zero average should be represented by a time-dependent moving average.

<sup>7</sup> For neutrino capture on polarized nuclei,  $A_0$  is only constant when the degree of polarization of the target nuclei does not change with time. Depolarization effects will lead to a decrease of  $A_0$  with time, and re-polarization of the target nuclei in the course of the experiment (or between the runs) may be necessary. Possible time dependence of  $A_0$  can be readily incorporated in the statistical treatment of the signal.

and similarly for the noise. The signal and noise power spectra  $S(\omega)$  and  $N(\omega)$  are the Fourier transforms of the corresponding autocorrelation functions:

$$S(\omega) = \int_{-\infty}^{\infty} d\tau e^{-i\omega\tau} R_{ss}(\tau), \quad N(\omega) = \int_{-\infty}^{\infty} d\tau e^{-i\omega\tau} R_{nn}(\tau). \quad (4.5)$$

If the power spectra are known, the autocorrelation functions can be obtained as inverse Fourier transforms:

$$R_{ss}(\tau) = \int_{-\infty}^{\infty} \frac{d\omega}{2\pi} e^{i\omega\tau} S(\omega), \quad R_{nn}(\tau) = \int_{-\infty}^{\infty} \frac{d\omega}{2\pi} e^{i\omega\tau} N(\omega). \quad (4.6)$$

Note that the power spectrum of the signal can also be found as

$$S(\omega) = \lim_{T \rightarrow \infty} \frac{1}{T} |\tilde{s}(\omega)|^2, \quad (4.7)$$

where  $\tilde{s}(\omega)$  is the Fourier transform of the time-dependent signal  $s(t)$ :

$$\tilde{s}(\omega) = \int_{-\infty}^{\infty} dt e^{-i\omega t} s(t). \quad (4.8)$$

This can be readily shown by substituting  $R_{ss}(\tau)$  from (4.4) into the first equation in (4.5).

The autocorrelation function of a periodic function of period  $T_0$  is itself a periodic function of the time lag  $\tau$  with the same period. In particular, for the sinusoidal periodic signal (4.3) we find

$$R_{ss}(\tau) = \frac{A_0^2}{2} \cos \omega_0 \tau. \quad (4.9)$$

The power spectrum of such a signal consists of two discrete lines corresponding to the frequencies  $\omega = \pm\omega_0$ :

$$S(\omega) = \frac{\pi}{2} A_0^2 \{ \delta(\omega - \omega_0) + \delta(\omega + \omega_0) \}. \quad (4.10)$$

The autocorrelation functions of random time distributions take their maximum values at  $\tau = 0$  and tend to zero as  $\tau \rightarrow \infty$ . In the case of interest to us, the noise  $n(t)$  is due to the fluctuations of the background event rate. As the values of these fluctuations at different times are completely statistically independent, all the frequencies contribute to the power spectrum of the noise with the same weight, i.e.

$$N(\omega) = N_0 = \text{const.} \quad (4.11)$$

Such random time distributions with flat power spectrum are called white noise. The corresponding autocorrelation function

$$R_{nn}(\tau) = N_0 \delta(\tau) \quad (4.12)$$

vanishes for all  $\tau \neq 0$ .

Within this approach it would be formally possible to separate arbitrarily weak periodic signal from noise: it would be sufficient to consider their autocorrelation functions at any non-zero time lag  $\tau$  satisfying  $\omega_0\tau \neq \pi/2 + \pi n$ . The noise autocorrelation function (4.12) would then vanish, while the signal autocorrelation function  $R_{ss}$  of eq. (4.9) would remain finite. This, however, would have only been the case for infinite  $T$ , whereas all experiments have finite duration. Another indication of the oversimplified nature of the above consideration is

that the total noise power obtained by integrating the flat power spectrum of eq. (4.11) over the whole frequency interval  $(-\infty, \infty)$  is infinite. The resolution comes from the observation that any realistic measurement actually has a finite bandwidth, i.e. is characterized by a finite interval of frequencies. We therefore turn now to the realistic case of finite total observation time  $T$  and finite measurement bandwidth.

In experiments with time-dependent signal, quite often time binning of the data is invoked, either because of the experimental conditions or basing on some statistical considerations. For the bin length  $\Delta t$ , the signal will then represent a finite discrete time series, similar to those obtained by sampling continuous signals with the sampling rate  $1/\Delta t$ . The bin length, however, cannot be too large: the lossless reconstruction of a signal is in general only possible if the sampling rate exceeds twice the maximal linear frequency contained in the signal [31–36]. For a simple periodic signal of period  $T_0$  this means that the sampling interval  $\Delta t$  must be below  $T_0/2$ .

For a time series with a uniform sampling interval  $\Delta t$  the bandwidth is limited by  $|\omega| \leq \omega_m$ , where the maximal frequency  $\omega_m$  is related to the Nyquist linear frequency  $f_N \equiv (2\Delta t)^{-1}$  by

$$\omega_m = 2\pi f_N = \frac{\pi}{\Delta t}. \quad (4.13)$$

This is essentially the highest frequency about which there is information, because  $\Delta t$  is the shortest time interval spanned. In the case of uneven sampling, when the lengths of the sampling intervals vary, a generalized Nyquist linear frequency can be introduced, defined as  $(2\Delta t)^{-1}$  with  $\Delta t$  being the mean sampling interval [36]. In experiments allowing real-time detection of the signal, binning of the data is not necessary and may actually be detrimental to detection of time-dependent signals [37], as any binning leads to information loss. In such real-time detection experiments  $\Delta t$  can be taken to be the mean time interval between two consecutive events, i.e. the reciprocal of the mean event rate.

Let us now consider the signal-to-noise ratio and its improvement by frequency-domain filtering, taking into account that the total observation time  $T$  is finite. In what follows we will be assuming  $\Delta t \ll T$  and for simplicity will replace the summation over the event detection times by integration, which corresponds to the limit  $\Delta t \rightarrow 0$ . The finite actual length of  $\Delta t$  will only be reflected in that the integration in the frequency domain will be limited by the interval  $[-\omega_m, \omega_m]$ . More refined approach would be to estimate the signal power spectrum by calculating periodograms based on discrete Fourier transform [35, 36]; however for our purpose of obtaining simple estimates the approach we adopt is quite adequate.

Let us first calculate the signal power spectrum. It can be shown that  $S(\omega)$  has the same form as that in eq. (4.7) except that no limit  $T \rightarrow \infty$  is taken and  $\tilde{s}(\omega)$  is now the finite-interval Fourier transform of  $s(t)$ . Direct calculation with  $s(t)$  from eq. (4.3) yields

$$\tilde{s}(\omega) = \int_{-T/2}^{T/2} dt e^{-i\omega t} s(t) = A_0 \left\{ -ie^{i\varphi} \frac{\sin [(\omega - \omega_0)\frac{T}{2}]}{\omega - \omega_0} + ie^{-i\varphi} \frac{\sin [(\omega + \omega_0)\frac{T}{2}]}{\omega + \omega_0} \right\}. \quad (4.14)$$

The power spectrum of the signal is then

$$S(\omega) = \frac{A_0^2}{T} \left\{ \frac{\sin^2 [(\omega - \omega_0)\frac{T}{2}]}{(\omega - \omega_0)^2} + \frac{\sin^2 [(\omega + \omega_0)\frac{T}{2}]}{(\omega + \omega_0)^2} - 2 \frac{\sin [(\omega - \omega_0)\frac{T}{2}]}{\omega - \omega_0} \frac{\sin [(\omega + \omega_0)\frac{T}{2}]}{\omega + \omega_0} \cos 2\varphi \right\}. \quad (4.15)$$

It contains two main peaks with the centers at  $\omega = \pm\omega_0$  (see fig. 1). The widths of each peak can be characterized by the distance between the two zeros nearest to the peak position;



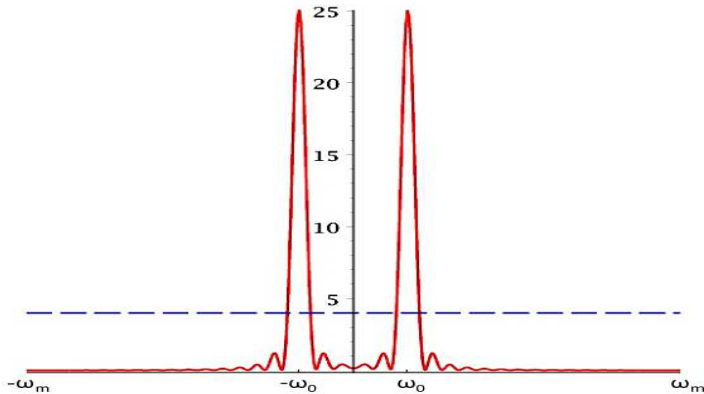


**Figure 1.** Schematic representation of the power spectra of the signal  $S(\omega)$  (red solid curve) and noise  $N(\omega)$  (blue dashed line).

this corresponds to the intervals  $\pm 2\pi/T$  around the centers of the peaks. Since the distance between the centers of the two main peaks  $2\omega_0$  is much larger than the width of the peaks  $4\pi/T$ ,<sup>8</sup> the peaks are practically non-overlapping, and one can safely neglect the cross-product term (the last term in the curly brackets) in eq. (4.15). The interval  $[-2\pi/T, 2\pi/T]$  around the center of each peak contains about 90% of its strength (see eq. (4.19) below). In the limit  $T \rightarrow \infty$  we recover the result in eq. (4.10).

It was pointed out above that the signal and noise strengths can be characterized by their variances,  $\overline{s(t)^2}$  and  $\overline{n^2(t)}$ . As follows from (4.4) and the similar definition of  $R_{nn}(\tau)$ , these variances coincide with the values of the corresponding autocorrelation functions at the origin, which in turn are given by the integrals of the signal and noise powers over the bandwidth  $\Omega$  of the measurement:

$$\overline{s(t)^2} = R_{ss}(0) = \int_{\Omega} \frac{d\omega}{2\pi} S(\omega), \quad \overline{n(t)^2} = R_{nn}(0) = \int_{\Omega} \frac{d\omega}{2\pi} N(\omega). \quad (4.16)$$

As the power spectrum of the background fluctuations  $N(\omega)$  is essentially constant throughout the bandwidth of the experiment  $[-\omega_m, \omega_m]$ , we have

$$\overline{n(t)^2} \equiv \sigma_0^2 = \int_{-\omega_m}^{\omega_m} \frac{d\omega}{2\pi} N(\omega) \simeq \frac{\omega_m}{\pi} N_0. \quad (4.17)$$

In the case under consideration, the noise is due to the statistical fluctuations of the background related to quantum nature of the underlying processes and discrete nature of the detected particles; this is a special case of white noise called shot noise [34]. The flat power spectrum of such a noise is given by the number of events per unit time (see e.g. [38] for a simple derivation). Thus, the quantity  $N_0$  in eq. (4.17) is just the mean background event rate.

We will now make use of the fact that the signal is concentrated in the narrow intervals in the frequency domain (which become narrower as the total observation time increases), whereas the noise power is constant per unit bandwidth. To improve the signal-to-noise ratio, we therefore integrate the signal and noise power spectra over the intervals  $\Delta\omega =$

<sup>8</sup>We assume that the total observation time  $T$  is much larger than the period of the sidereal daily variations of the signal  $2\pi/\omega_0 \simeq 24$  h.

$[-2\pi/T, 2\pi/T]$  around the points  $\omega = \pm\omega_0$ . Since the regions around these two points give identical contributions to the signal power as well as to the noise power, for the ratio it is sufficient to consider only one such region. We therefore define the improved signal-to-noise ratio as

$$\rho = \frac{\int_{\Delta\omega} \frac{d\omega}{2\pi} S(\omega)}{\int_{\Delta\omega} \frac{d\omega}{2\pi} N(\omega)}. \quad (4.18)$$

With the expression for  $S(\omega)$  from eq. (4.15) and  $N(\omega) = N_0$  we find

$$\int_{\Delta\omega} \frac{d\omega}{2\pi} S(\omega) \simeq \frac{A_0^2}{4\pi} \int_{-\pi}^{\pi} \frac{\sin^2 x}{x^2} dx = \frac{A_0^2}{4} \frac{2\text{Si}(2\pi)}{\pi} \simeq \frac{A_0^2}{4} \cdot 0.9028, \quad (4.19)$$

$$\int_{\Delta\omega} \frac{d\omega}{2\pi} N(\omega) \simeq \frac{2N_0}{T}. \quad (4.20)$$

Substituting this into eq. (4.18) yields

$$\rho \simeq \frac{0.9028 A_0^2 T}{8N_0}. \quad (4.21)$$

This quantity essentially coincides (up to about a factor of 1/2) with the ratio of the peak value of the signal power to the (flat) value of the noise power. Comparing this result with the original signal-to-noise ratio  $s(t)^2/n(t)^2$  that may be found by integrating the signal and noise power spectra over the full interval  $[-\omega_m, \omega_m]$ , we find that the improvement factor due to the passband filtering is about  $0.225N_0T$ . As  $N_0T$  is the number of background events detected over the total observation time  $T$ , this factor can be quite large.

An alternative interpretation of the obtained result can be given by comparing it with the signal-to-background ratio rather than with the “un-filtered” signal-to-noise one. To this end, let us rewrite eq. (4.21) as

$$\rho \simeq \frac{(A_0/\sqrt{2})T}{N_0T} \cdot \left[ 0.225(A_0T/\sqrt{2}) \right]. \quad (4.22)$$

Here the quantity  $(A_0/\sqrt{2})T$  is the root mean square number of the “signal events” (i.e. of the events caused by the periodic component of the neutrino capture signal) over the time interval  $T$ . The first factor in eq. (4.22) is therefore essentially the signal-to-background ratio. The expression in the square brackets is the enhancement factor, which increases with increasing signal statistics  $(A_0/\sqrt{2})T$ .

From eq. (4.22) it can be seen that, though the noise reduction by simple frequency-domain filtering considered here will greatly improve the signal-to-noise ratio, it will not be sufficient for a reliable signal detection unless the total number of the detected signal events is very large. Indeed, for  $\delta \sim 0.1$  eV and  $u \sim 10^{-3}$  the signal-to-background ratio is expected to be of order  $2.5 \times 10^{-11}$ . Thus, with the simple frequency-domain filtering discussed above, an unrealistically large number of signal events ( $\gtrsim 2.5 \times 10^{11}$ ) would be necessary in order to detect the  $C\nu\text{B}$  signal. Therefore, more sophisticated methods of noise reduction must be invoked. As an example, the signal-to-noise ratio can be further improved by measuring the noise power spectrum in the frequency regions where the signal is essentially absent (i.e. away from the neighborhoods of  $\omega = \pm\omega_0$ ) in order to predict its value in the regions where the signal is concentrated and cancel (subtract) it there [39]. The cancellation will, however, be incomplete as the noise spectrum is in reality only approximately flat.

Preliminary estimates show that such noise cancellation may reduce the requisite number of signal events to about  $10^4$ . Other methods of noise suppression can also be used, such as e.g. studying cross-correlation of the observed data with test functions in the form of the expected time-dependent signal, as it is currently done in gravitational wave detection.

To be able to make a more definitive statement on the possibility of noise suppression, one would need to perform signal and noise simulations in the conditions of a particular experiment.

## 5 Discussion

We have suggested an alternative method of detection of  $C\nu B$  through neutrino capture on beta-decaying nuclei, based on observation of time variations of the total detection rates or of various angular correlations characteristic of  $\beta$ -processes. The time dependence should come about because of the peculiar motion of the Sun with respect to  $C\nu B$  and rotation of the Earth about its axis. The variations of total  $C\nu B$  detection rate can be observed in experiments with polarized nuclear targets, whereas the observation of modulated  $\beta - \nu$  angular correlation or of the correlation between the neutrino direction and the spin of the produced electron does not require target polarization. As an example, we considered neutrino detection through allowed Gamow-Teller  $1^\pi \rightarrow 0^\pi$   $\beta$ -transitions; however, our results can be readily generalized to arbitrary allowed Gamow-Teller transitions  $J^\pi \rightarrow J^\pi \pm 1$ .

One advantage of pure Gamow-Teller transitions is that the effects of the target polarization are more prominent in this case. Consider e.g. pure Gamow-Teller  $J^\pi \rightarrow J^\pi - 1$  transitions (of which the  $1^\pi \rightarrow 0^\pi$  process we have studied is an example). In this case the detection cross section will be exactly zero if the incoming neutrino is in a helicity eigenstate and its spin is aligned with that of the parent nucleus. Indeed, in this case the total angular momentum of the initial state (incoming neutrino + parent nucleus) is  $J + 1/2$ ; due to angular momentum conservation, such a system cannot decay into a daughter nucleus with spin  $J - 1$  and electron. Likewise, the probability of the process vanishes if the produced electron is in a helicity eigenstate with its spin antialigned with the polarization of the parent nucleus. It is easy to see that our squared amplitude (2.10) satisfies these conditions (see footnote 2). The case of pure Gamow-Teller  $J^\pi \rightarrow J^\pi + 1$  transitions can be considered quite similarly.

On the other hand, pure Fermi transitions  $0^\pi \rightarrow 0^\pi$  may be useful for observing  $\beta - \nu$  angular correlations in relic neutrino capture on unpolarized nuclei, as they are characterized by a sizeable correlation coefficient  $a = 1$ . An important advantage of pure transitions is that for them the angular correlations coefficients do not depend on nuclear matrix elements.

For the non-relativistic component of  $C\nu B$ , the coefficients of angular correlations in relic neutrino capture are different for Dirac and Majorana neutrinos, and so one might hope that observing these correlations would help establish neutrino nature. Unfortunately, this would be extremely difficult, as the differences between the correlation coefficients for Dirac and Majorana neutrinos are additionally suppressed by the small factor  $v_j$ .

The suggested method of  $C\nu B$  detection is obviously prone to difficulties. One of them is related to the expected smallness of the amplitude of the periodic variation of the relic neutrino signal. It will therefore be necessary to extract a weak periodic signal from a large fluctuating background of electrons or positrons from the usual  $\beta$ -decay. In experiments with polarized nuclear targets one will also have to face experimental problems related with the requirement of polarization of the target nuclei and maintaining this polarization for an extended period of time (or renewing it in the course of the experiment).

On the other hand, there are well-developed powerful methods of signal-from-noise separation, which are especially efficient when the signal is of known periodicity and which therefore may be helpful in solving the problem of detecting relic neutrinos through time variations of their signal. The  $C\nu B$  detection may also be facilitated by the fact that there exist several independent angular correlations which are expected to exhibit time variations of the same periodicity. It is also worth noticing that the the angular correlations in the relic neutrino capture may be enhanced in the presence of non-standard neutrino physics, such as relatively large neutrino magnetic moments [18].

The main advantage of the approach suggested in this paper is that it does not in principle require extremely high energy resolution of the detector. Good energy resolution would certainly be helpful, as it would allow one to suppress the background of electrons or positrons coming from the competing  $\beta$  decay by working close to the endpoint of their spectrum. However, the method can still be operative even for relatively large energy resolution, if sufficiently potent method of separation of the weak periodic signal from strong random noise is employed. This is in contrast with the situation with the usually considered method of relic neutrino detection based on the separation of the spectra of  $\beta$ -particles from neutrino absorption and  $\beta$  decay. The latter would not work if the energy resolution of the detector exceeds the largest neutrino mass. The fact that the requirements on the energy resolution are less severe in the approach suggested here, in particular, means that radioactive nuclei with relatively large  $Q_\beta$  values may be preferable as target, because they lead to larger absolute detection rates.

Much work has yet to be done to establish if the approach to  $C\nu B$  detection suggested in this paper is actually feasible, including selection of suitable nuclides (taking into account, among other aspects, their availability, lifetime, type of  $\beta$  transition, (neutrino capture)/( $\beta$  decay) rate ratio and feasibility of target polarization in the case of experiments with polarized nuclei). Extensive simulations of the signal and background will also be necessary to clarify if the proposed  $C\nu B$  detection method is actually viable and is competitive with the approach based on the separation of the spectra of  $\beta$ -particles from relic neutrino capture from those produced in  $\beta$  decay of target nuclei.

## Acknowledgments

The author is grateful to Alexei Smirnov for numerous useful discussions and to Eligio Lisi for useful correspondence.

## A Angular averaging

We will consider here the effects of averaging over the angular distributions of relic neutrinos on the angular correlations of interest in the lab frame. We will be assuming that in the  $C\nu B$  rest frame neutrinos have isotropic velocity distribution and are in the exact helicity eigenstates; therefore their spins are also distributed isotropically. As in section 3, we will use the unprimed notation for the neutrino variables in the  $C\nu B$  rest frame, whereas the primed quantities will refer to the lab frame, moving with the velocity  $-\vec{u}$  with respect to the cosmic one. We will consider the effects of Lorentz boost from the  $C\nu B$  rest frame to the lab frame to first order in  $u$ . The neutrino energy, momentum and velocity in the lab frame are given in eq. (3.1). The expressions for neutrino spin in the lab frame are given in eq. (3.3) in the general case and in eq. (3.5) for neutrinos that are in helicity eigenstates in the  $C\nu B$

rest frame. It was demonstrated in section 3 that in the case  $v_j \gg u$  of main interest to us neutrinos that were in states of definite helicity in the CνB frame will remain in the same helicity states in the lab frame up to corrections  $\mathcal{O}(u^2)$  which we neglect.

From eqs. (3.1) and (3.5) we find

$$\vec{v}'_j \cdot \vec{s}'_j = \lambda_j v_j \left\{ 1 + (\vec{u} \cdot \vec{v}_j) \frac{1 - v_j^2}{v_j^2} \right\}. \quad (\text{A.1})$$

For the quantity  $K_j$  that enters into the expression for the neutrino vector  $B^\mu$  we then obtain in the lab frame

$$K'_j = 1 - \frac{E'_j}{E'_j + m_j} (\vec{v}'_j \cdot \vec{s}'_j) = 1 - \frac{E_j}{E_j + m_j} \lambda_j v_j \left( 1 + \frac{\vec{u} \cdot \vec{v}_j}{v_j^2} \frac{m_j}{E_j} \right). \quad (\text{A.2})$$

This gives

$$\frac{1}{E'_j} \vec{B}' = K'_j \vec{v}'_j - \frac{m_j}{E'_j} \vec{s}'_j = (1 - \lambda_j v_j) \left\{ \vec{u} - (1 - \vec{u} \cdot \vec{v}_j) \lambda_j \frac{\vec{v}_j}{v_j} \right\}. \quad (\text{A.3})$$

Consider now the effects of averaging over the angular distributions of relic neutrinos on neutrino variables, taking into account that neutrino velocity and spin distributions in the CνB rest frame are isotropic. Denoting the averaging over the directions by angular brackets and taking into account that  $\langle \vec{v}_j \rangle = 0$  and  $\langle \vec{s}_j \rangle = 0$ , for the quantities in the lab frame we find

$$\langle E'_j \rangle = E_j, \quad \langle \vec{q}' \rangle = \vec{u} E_j, \quad \langle \vec{v}'_j \rangle = \left( 1 - \frac{v_j^2}{3} \right) \vec{u}, \quad (\text{A.4})$$

$$\left\langle \frac{\vec{v}'_j}{v'_j} \right\rangle = \frac{2}{3} \frac{\vec{u}}{v_j}, \quad (\text{A.5})$$

$$\langle \vec{s}'_j \rangle = \lambda_j v_j \frac{2}{3} \frac{E_j}{E_j + m_j} \vec{u}, \quad \langle \vec{v}'_j \cdot \vec{s}'_j \rangle = \lambda_j v_j = \langle \vec{v}_j \cdot \vec{s}_j \rangle. \quad (\text{A.6})$$

This yields

$$\left\langle \frac{1}{E'_j} B^{0'} \right\rangle = 1 - \langle \vec{v}'_j \cdot \vec{s}'_j \rangle = 1 - \lambda_j v_j, \quad (\text{A.7})$$

$$\left\langle \frac{1}{E'_j} \vec{B}' \right\rangle = \left\langle K'_j \vec{v}'_j - \frac{m_j}{E'_j} \vec{s}'_j \right\rangle = \left( 1 - \frac{2}{3} \lambda_j v_j - \frac{v_j^2}{3} \right) \vec{u}. \quad (\text{A.8})$$

With these relations, one readily obtains the expressions for the squared amplitude of the process given in sections 3.1 and 3.2.

## B Electron asymmetry with respect to a fixed direction in the lab frame

As discussed in section 3.2, the angular correlation between the direction of the produced electron and the preferred direction of the neutrino arrival in the case of relic neutrino capture on unpolarized nuclei can be written as

$$\text{const.} (1 + \alpha \vec{u} \cdot \vec{v}_e), \quad (\text{B.1})$$

where  $\alpha$  is the correlation coefficient (see eq. (3.14)). We want to find the time-dependent forward-backward asymmetry of electron emission with respect to a fixed direction in the lab frame specified by a unit vector  $\vec{\xi}$ . It is easy to see that the asymmetry would not depend on time for  $\vec{\xi}$  collinear with the rotation axis of the Earth and its time dependence will be maximized for orthogonal directions. We therefore choose  $\vec{\xi}$  to lie in the plane orthogonal to the Earth's rotation axis. In the geocentric spherical coordinates we have

$$\vec{u} = u(\cos \phi_u(t) \sin \theta_u, \sin \phi_u(t) \sin \theta_u, \cos \theta_u), \quad (\text{B.2})$$

$$\vec{v}_e = v_e(\cos \phi_e \sin \theta_e, \sin \phi_e \sin \theta_e, \cos \theta_e), \quad (\text{B.3})$$

$$\vec{\xi} = (\cos \phi_\xi, \sin \phi_\xi, 0), \quad (\text{B.4})$$

where

$$\phi_u(t) = \frac{2\pi}{T_0}t + \phi_0 \quad (\text{B.5})$$

and  $T_0 \simeq 24$  h is the sidereal day. From B.2 and B.3 we find

$$\vec{u} \cdot \vec{v}_e = uv_e [\cos \theta_u \cos \theta_e + \sin \theta_u \sin \theta_e \cos[\phi_u(t) - \phi_e]]. \quad (\text{B.6})$$

Straightforward calculation then gives for the forward-backward asymmetry of the electron emission with respect to  $\vec{\xi}$

$$\mathcal{A} \equiv \frac{\sigma_\uparrow - \sigma_\downarrow}{\frac{1}{2}[\sigma_\uparrow + \sigma_\downarrow]} = \alpha uv_e \sin \theta_u \cos[\phi_u(t) - \phi_\xi]. \quad (\text{B.7})$$

The electron spin asymmetry with respect to a fixed direction in the lab frame can be considered quite similarly.

## References

- [1] A. D. Dolgov, ‘‘Neutrinos in cosmology,’’ Phys. Rept. **370** (2002) 333 [hep-ph/0202122].
- [2] J. Lesgourgues and S. Pastor, ‘‘Massive neutrinos and cosmology,’’ Phys. Rept. **429**, 307 (2006) [astro-ph/0603494].
- [3] C. Quigg, ‘‘Cosmic neutrinos,’’ arXiv:0802.0013 [hep-ph].
- [4] T. J. Weiler, ‘‘Relic neutrinos, Z-bursts, and cosmic rays above  $10^{20}$  eV,’’ in Proc. *Beyond the Desert 99*, Tegernsee, Germany, 1999, edited by H. Klapdor-Kleingrothaus and I. Krivosheina, IoP Publishing, Bristol, 2000 [hep-ph/9910316].
- [5] G. B. Gelmini, ‘‘Prospect for relic neutrino searches,’’ Phys. Scripta T **121** (2005) 131 [hep-ph/0412305].
- [6] A. Ringwald, ‘‘Prospects for the direct detection of the cosmic neutrino background,’’ Nucl. Phys. A **827** (2009) 501C [arXiv:0901.1529 [astro-ph.CO]].
- [7] P. Vogel, ‘‘How difficult it would be to detect cosmic neutrino background?,’’ AIP Conf. Proc. **1666** (2015) no.1, 140003.
- [8] S. Weinberg, ‘‘Universal neutrino degeneracy,’’ Phys. Rev. **128** (1962) 1457.
- [9] A. G. Cocco, G. Mangano and M. Messina, ‘‘Probing low energy neutrino backgrounds with neutrino capture on beta decaying nuclei,’’ JCAP **0706** (2007) 015 [hep-ph/0703075].
- [10] R. Lazauskas, P. Vogel and C. Volpe, ‘‘Charged current cross section for massive cosmological neutrinos impinging on radioactive nuclei,’’ J. Phys. G **35** (2008) 025001 [arXiv:0710.5312 [astro-ph]].

- [11] M. Blennow, “Prospects for cosmic neutrino detection in tritium experiments in the case of hierarchical neutrino masses,” *Phys. Rev. D* **77** (2008) 113014 [arXiv:0803.3762 [astro-ph]].
- [12] A. G. Cocco, G. Mangano and M. Messina, “Low energy antineutrino detection using neutrino capture on EC decaying nuclei,” *Phys. Rev. D* **79** (2009) 053009 [arXiv:0903.1217 [hep-ph]].
- [13] Y. F. Li, Z. z. Xing and S. Luo, “Direct detection of the cosmic neutrino background including light sterile neutrinos,” *Phys. Lett. B* **692** (2010) 261 [arXiv:1007.0914 [astro-ph.CO]].
- [14] M. Lusignoli and M. Vignati, “Relic antineutrino capture on  $^{163}\text{Ho}$  decaying nuclei,” *Phys. Lett. B* **697** (2011) 11 Erratum: [*Phys. Lett. B* **701** (2011) 673] [arXiv:1012.0760 [hep-ph]].
- [15] A. Faessler, R. Hodak, S. Kovalenko and F. Simkovic, “Beta decaying nuclei as a probe of cosmic neutrino background,” arXiv:1102.1799 [hep-ph].
- [16] B. R. Safdi, M. Lisanti, J. Spitz and J. A. Formaggio, “Annual modulation of cosmic relic neutrinos,” *Phys. Rev. D* **90** (2014) no.4, 043001 [arXiv:1404.0680 [astro-ph.CO]].
- [17] A. J. Long, C. Lunardini and E. Sabancilar, “Detecting non-relativistic cosmic neutrinos by capture on tritium: phenomenology and physics potential,” *JCAP* **1408** (2014) 038 [arXiv:1405.7654 [hep-ph]].
- [18] M. Lisanti, B. R. Safdi and C. G. Tully, “Measuring anisotropies in the cosmic neutrino background,” *Phys. Rev. D* **90** (2014) no.7, 073006 [arXiv:1407.0393 [astro-ph.CO]].
- [19] E. Roulet and F. Vissani, “On the capture rates of big bang neutrinos by nuclei within the Dirac and Majorana hypotheses,” *JCAP* **1810** (2018) no.10, 049 [arXiv:1810.00505 [hep-ph]].
- [20] J. Y. Lee, Y. Kim and S. Chiba, “New targets for relic antineutrino capture,” arXiv:1811.05183 [hep-ph].
- [21] S. Betts *et al.*, “Development of a relic neutrino detection experiment at PTOLEMY: Princeton Tritium Observatory for Light, Early-universe, Massive-neutrino Yield,” arXiv:1307.4738 [astro-ph.IM].
- [22] M. G. Betti *et al.* [PTOLEMY Collaboration], “Neutrino physics with the PTOLEMY project,” arXiv:1902.05508 [astro-ph.CO].
- [23] E. Baracchini *et al.* [PTOLEMY Collaboration], “PTOLEMY: A proposal for thermal relic detection of massive neutrinos and directional detection of MeV dark matter,” arXiv:1808.01892 [physics.ins-det].
- [24] P. F. de Salas, D. V. Forero, C. A. Ternes, M. Tortola and J. W. F. Valle, “Status of neutrino oscillations 2018:  $3\sigma$  hint for normal mass ordering and improved CP sensitivity,” *Phys. Lett. B* **782** (2018) 633 [arXiv:1708.01186 [hep-ph]].
- [25] F. Capozzi, E. Lisi, A. Marrone and A. Palazzo, “Current unknowns in the three neutrino framework,” *Prog. Part. Nucl. Phys.* **102** (2018) 48 [arXiv:1804.09678 [hep-ph]].
- [26] I. Esteban, M. C. Gonzalez-Garcia, A. Hernandez-Cabezudo, M. Maltoni and T. Schwetz, “Global analysis of three-flavour neutrino oscillations: synergies and tensions in the determination of  $\theta_{23}$ ,  $\delta_{CP}$ , and the mass ordering,” *JHEP* **1901** (2019) 106 [arXiv:1811.05487 [hep-ph]].
- [27] J. D. Jackson, S. B. Treiman and H. W. Wyld, “Possible tests of time reversal invariance in beta decay,” *Phys. Rev.* **106** (1957) 517.
- [28] J. D. Jackson, S. B. Treiman and H. W. Wyld, “Coulomb corrections in allowed beta transitions,” *Nucl. Phys.* **4** (1957) 206.
- [29] M. Goldhaber, L. Grodzins and A. W. Sunyar, “Helicity of neutrinos,” *Phys. Rev.* **109** (1958) 1015.
- [30] P. F. de Salas, S. Gariazzo, J. Lesgourgues and S. Pastor, “Calculation of the local density of relic neutrinos,” *JCAP* **1709** (2017) no.09, 034 [arXiv:1706.09850 [astro-ph.CO]].

- [31] L. A. Wainstein and V. D. Zubakov, *Extraction of Signal from Noise*, Dover, New York, 1970.
- [32] J. G. Proakis and D. G. Manolakis, *Digital Signal Processing*, Prentice Hall, 1996.
- [33] D. R. Brillinger, *Time Series. Data Analysis and Theory*, SIAM, Philadelphia, 2001.
- [34] A. Papoulis and S. U. Pillai, *Probability, random variables, and stochastic processes*, 4th ed., McGraw-Hill, New York, 2002.
- [35] N. R. Lomb, “Least - squares frequency analysis of unequally spaced data,” *Astrophys. Space Sci.* **39** (1976) 447.
- [36] J. D. Scargle, “Studies in astronomical time series analysis. 2. Statistical aspects of spectral analysis of unevenly spaced data,” *Astrophys. J.* **263** (1982) 835.
- [37] E. Lisi, A. Palazzo and A. M. Rotunno, “Unbinned test of time dependent signals in real time neutrino oscillation experiments,” *Astropart. Phys.* **21** (2004) 511 [hep-ph/0403036].
- [38] X. Chen, “On Schottky noise and shot noise,” arXiv:1805.12207 [physics.ins-det].
- [39] J. Samsing, “Extracting periodic transit signals from noisy light curves using Fourier series”, *Astrophys. J.* **807** (2015) 65, arXiv:1503.03504 [astro-ph.EP].